



Noble gas isotopic compositions of mantle xenoliths from northwestern Pacific lithosphere

Junji Yamamoto^{a,b,*}, Naoto Hirano^c, Natsue Abe^d, Takeshi Hanyu^d

^a Woods Hole Oceanographic Institution, Woods Hole, MA 02543, USA

^b Institute for Geothermal Sciences, Kyoto University, Noguchibaru, Beppu 874-0903, Japan

^c Center for Northeast Asian Studies, Tohoku University, 41 Kawauchi, Aoba-ku, Sendai 980-8576, Japan

^d Institute for Research on Earth Evolution (IFREE), Independent Administrative Institution/Japan Agency for Marine–Earth Science and Technology (JAMSTEC), 2-15 Natsushima, Yokosuka 237-0061, Japan

ARTICLE INFO

Article history:

Received 20 April 2009

Received in revised form 4 September 2009

Accepted 8 September 2009

Editor: R.L. Rudnick

Keywords:

Noble gases
Diffusive fractionation
Petit-spot volcano
Mantle xenolith
Xenocryst

ABSTRACT

We measured noble gas isotopic compositions of mantle xenoliths and xenocrystic olivines sampled from seamounts—so-called petit-spot volcanoes—on the 135-million-year-old northwestern Pacific Plate. The xenoliths are spinel lherzolites originating from suboceanic lithospheric mantle. The samples' $^3\text{He}/^4\text{He}$ ratios are 7.0–8.5 Ra, where Ra signifies atmospheric $^3\text{He}/^4\text{He}$. The $^{40}\text{Ar}/^{36}\text{Ar}$ ratios are as high as 7000. These observations suggest that the noble gas isotopic compositions of suboceanic lithospheric mantle resemble those of mid-ocean ridge basalt (MORB). A mantle source with a He/U ratio as high as an assumed value for MORB source is necessary to maintain the MORB-like $^3\text{He}/^4\text{He}$ over 135 million years, implying that melt extraction at mid-ocean ridges only slightly alters the He/U ratio of the oceanic upper mantle.

The $^4\text{He}/^{40}\text{Ar}^*$ ratios of the samples described herein are much lower than the theoretical radiogenic production ratio, where an asterisk denotes correction for atmospheric contribution. The low $^4\text{He}/^{40}\text{Ar}^*$ is inferred to result from kinetic fractionation in the mantle. When magma migrates through a mantle source, lighter noble gases in the mantle source diffuse selectively into magma channels. The MORB generation does not cause low $^4\text{He}/^{40}\text{Ar}^*$, however. If a mantle source is depleted in lighter noble gases during ancient MORB generation, then noble gas isotopic compositions of the mantle source are affected over time by accumulation of radiogenic nuclides. Thereby, the mantle source adopts a radiogenic or nucleogenic noble gas isotopic composition. Recent kinetic fractionation contributes to the low $^4\text{He}/^{40}\text{Ar}^*$ in the samples. Based on the diffusive fractionation model, more than 100 years are necessary to produce a residual mantle source with $^4\text{He}/^{40}\text{Ar}^*$, as observed in the samples. However, petit-spot volcanoes, found as small knolls, seem to erupt within a short period. The low $^4\text{He}/^{40}\text{Ar}^*$ of the samples implies prior volcanism in this region. No recent volcanism has occurred near this region aside from petit-spot volcanism, indicating that petit-spot volcanoes are polygenetic with a long active period.

Petit-spot volcanoes are regarded as common magmatism on the subducting oceanic plate. Consequently, the thermal structure and temperature-dependent physical properties of the oceanic plate are, at least partly, affected by remnant heat of the magmatism.

© 2009 Elsevier B.V. All rights reserved.

1. Introduction

The $^3\text{He}/^4\text{He}$ of MORB shows a uniform value of 8.75 ± 2.14 Ra (Graham, 2002). Often, MORB-like $^3\text{He}/^4\text{He}$ has been observed in mantle-derived rocks from the subcontinental lithospheric mantle (SCLM) (Matsumoto et al., 1998, 2000, 2001; Dodson and Brandon, 1999; Hopp et al., 2004, 2007a; Yamamoto et al., 2004; Buikin et al., 2005; Kim et al., 2005; Gautheron et al., 2005; Czuppon et al., 2009). A widespread consensus holds that the source of MORB is a ubiquitous component of

the upper mantle (e.g., Matsumoto et al., 1998; Yamamoto et al., 2004). However, noble gas isotopic compositions of most parts of the suboceanic lithospheric mantle (SOLM) remain to be elucidated. What noble gas isotopic composition should the SOLM have after MORB extraction? Recent experimental measurements to determine partition coefficients of He suggest that mantle melting enhances the He/U ratio of the residual mantle (Parman et al., 2005; Heber et al., 2007), which allows preservation of MORB-like $^3\text{He}/^4\text{He}$ of the SOLM over time.

Peridotite xenoliths sampled at ocean islands offer a key to clarification of noble gas isotopic compositions of the SOLM. Many reports of noble gas isotopic compositions of oceanic peridotite xenoliths, however, specifically describe dunites or harzburgites, which could be of cumulate origin. Three reports describe noble gas isotopic compositions of

* Corresponding author. Woods Hole Oceanographic Institution, Woods Hole, MA 02543, USA. Tel.: +1 508 289 3658; fax: +1 508 457 2193.

E-mail address: jjyamamoto@whoi.edu (J. Yamamoto).

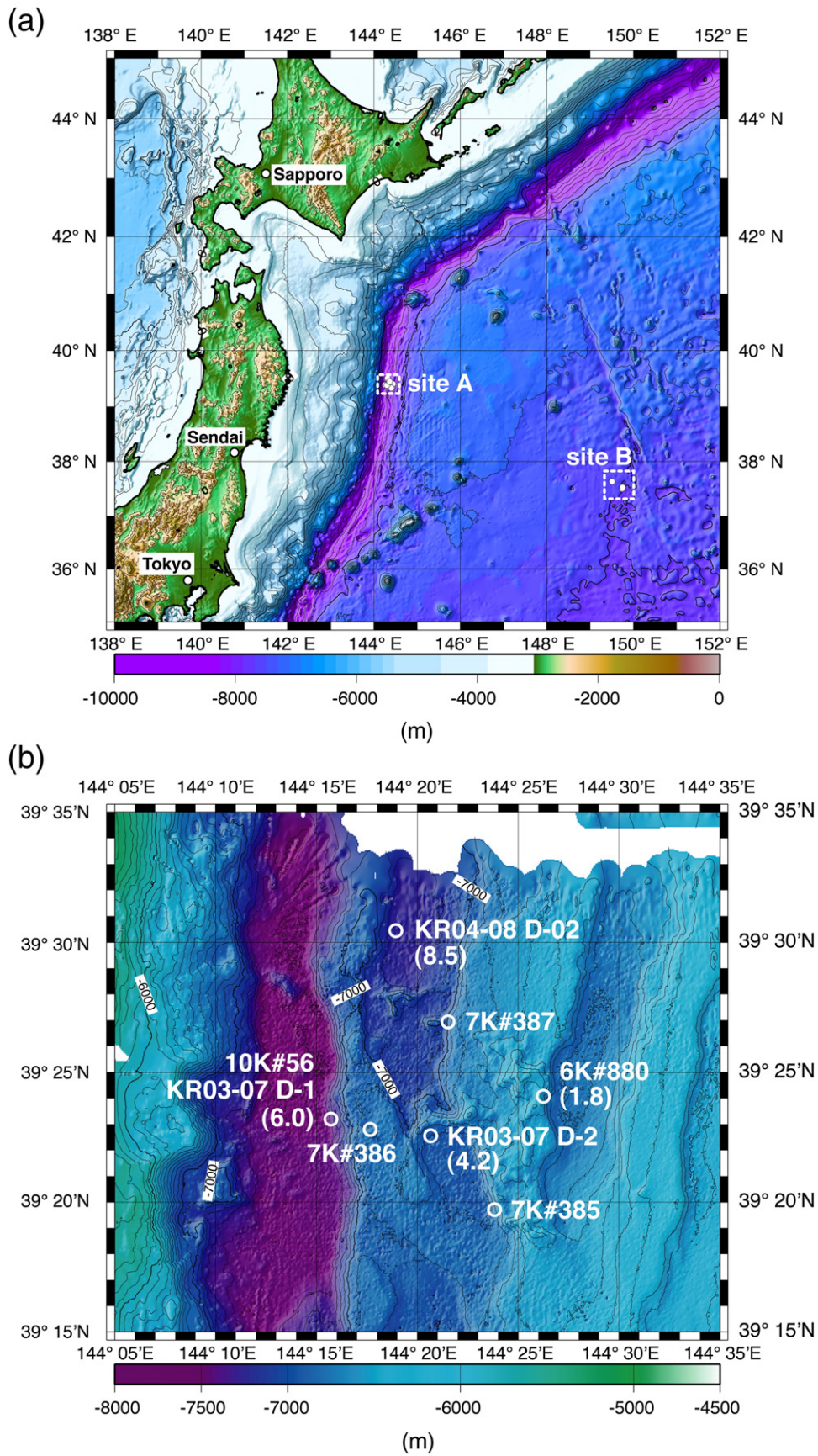


Fig. 1. (a) Map of the northwestern Pacific Ocean. Surveyed areas (sites A and B) are depicted as boxes. (b) Map of site A with open circles indicating sampling points of 6K#880, KR03-07 and 10K#56, and the other petit-spot volcanoes. (c) Map of site B with open circles showing sampling points of 6K#878 and the other petit-spot volcanoes whose eruption ages are less than 1 Ma (Hirano et al., 2006). Eruption ages (Ma) are in parentheses. Topographic data are from Amante and Eakins (2008).

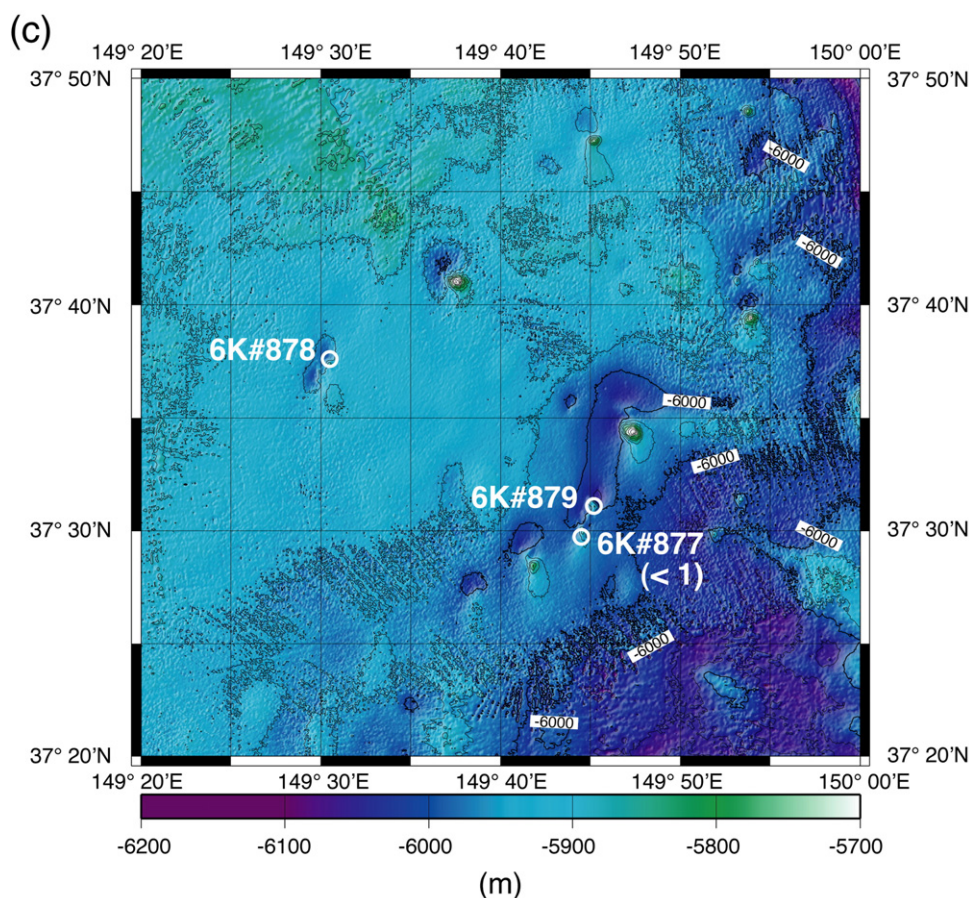


Fig. 1 (continued).

spinel-lherzolite xenoliths from oceanic islands (Kaneoka and Takaoka, 1980; Kyser and Rison, 1982; Vance et al., 1989). They applied a heating method to extract noble gases, which include secondary generated nuclides such as cosmogenic and radiogenic nuclides. Vance et al. (1989) analyzed $^3\text{He}/^4\text{He}$ of six oceanic lherzolite xenoliths also by crushing extraction. That study obtained MORB-like $^3\text{He}/^4\text{He}$ (8.4–9.5 Ra) from five Hawaiian lherzolite xenoliths and slightly lower $^3\text{He}/^4\text{He}$ (6.6 Ra) from a lherzolite xenolith from the Canary Islands, where the islands are underlain by the 155–175 Ma old oceanic plate (Neumann et al., 2000). Kumagai et al. (2003) reported MORB-like $^3\text{He}/^4\text{He}$ (8.3 Ra) of olivine grains in an abyssal lherzolite recovered from the youngest oceanic plate (Southwest Indian Ridge). These results imply possible accumulation of radiogenic ^4He within the old oceanic plate. However, at the present stage, noble gas isotopic compositions of the old oceanic plate, far from spreading centers, are represented by only one sample from the Canary Islands (Vance et al., 1989). In addition, because lherzolite xenoliths in the Canary Islands are well known for evident traces of carbonatite metasomatism (Neumann and Wulff-Pedersen, 1997; Klügel, 1998; Neumann et al., 2002), little is known about pristine features of noble gas isotopic compositions of the SOLM.

Some alkali basalts containing lherzolite xenoliths were discovered at volcanoes on the 135-million-year-old northwestern Pacific Plate (Hirano et al., 2006; Abe et al., 2006). Some lherzolite xenoliths were sufficiently large for noble gas isotopic analysis. Herein, we report isotopic compositions of their noble gases, which were extracted using the crushing method.

2. Samples

Young alkali basalts have been discovered on the northwestern Pacific Plate (Fig. 1). Called petit-spot volcanoes, they are reportedly a new form

of intra-plate volcanism related to plate flexure off the forebulge of the subducting Pacific Plate (Hirano et al., 2001, 2004, 2006). The basalts show light rare-earth element (REE)-enriched curves in primitive mantle-normalized REE patterns (Hirano et al., 2001, 2006), which support the assumption that the petit-spot magmatism is derived from minor extents of asthenospheric melting (Hirano et al., 2006).

During a survey of the area by the Japan Agency for Marine–Earth Science and Technology (JAMSTEC) research vessel KAIREI and support vessel YOKOSUKA during KR97-11, KR03-07, KR04-08 and YK05-06 cruises, basaltic rocks containing peridotite xenoliths were recovered from the petit-spot volcanoes by dredging and by use of the manned research submersibles SHINKAI 6500 and ROV KAIKO 10000.

Table 1
Sampling points of mantle xenoliths and xenocrysts from northwestern Pacific plate.

Dredge no. (dive no.)	Samples	Eruption age Ma	Depth m	Latitude	Longitude	Site
<i>Xenoliths</i>						
6K#878	2As	<1.0?	5902	37°37.4956'N	149°30.3865'E	B
6K#878	2Aa	<1.0?	5902	37°37.4956'N	149°30.3865'E	B
6K#878	2Al	<1.0?	5902	37°37.4956'N	149°30.3865'E	B
6K#880	2A	1.8	6474	39°23.7779'N	144°26.2896'E	A
6K#880	2D	1.8	6474	39°23.7779'N	144°26.2896'E	A
<i>Xenocrysts</i>						
KR03-07	D2-502a	4.2	6955	39°22.5571'N	144°20.6616'E	A
KR03-07	D2-502b	4.2	6955	39°22.5571'N	144°20.6616'E	A
<i>Xenocrysts (after Yamamoto et al. (2003))</i>						
10K#56	R1 (crushing)	6.0	7360	39°23.1173'N	144°15.6582'E	A
10K#56	R1 (heating)	6.0	7360	39°23.1173'N	144°15.6582'E	A

The basalts were recovered from two sites: A and B (Fig. 1(a)). Information about sampling sites is presented in Table 1. At site A, petit-spot volcanoes are distributed exclusively within a 10 km radius (Fig. 1(b)). The oldest volcano at this site erupted 8.5 ± 0.2 Ma (Hirano et al., 2008) at the north end of site A. The eruption age of the oldest petit-spot volcano at the center of distribution in site A is 6.0 ± 0.3 Ma (Hirano et al., 2001). Xenocrystic olivines (sample R1) were recovered from the volcano (Hirano et al., 2004). Noble gas isotopic compositions of the xenocrysts were reported by Yamamoto et al. (2003). The second oldest petit-spot volcano around the center of the distribution erupted 4.2 ± 0.2 Ma (Hirano et al., 2006); it is located 7 km east of the former volcano. Xenocrystic olivines (samples D2-502a and D2-502b) were recovered from the volcano. Another volcano, this one with five sheets of lava flow, was discovered 9 km east–northeast of the volcano. We found peridotite xenoliths (samples 2A and 2D) in the second lava sheet from the top of the volcano. The eruption age of the third lava sheet is 1.8 ± 0.6 Ma (Hirano et al., 2008). The eruption stage of the second lava sheet cannot be ascertained because the third lava sheet is potentially dyke. Nevertheless, the lava sheets are expected to have derived from the latest volcanism at the site because a young eruption age is expected from volcanoes located distant from the Japan Trench, according to a hypothesis related to petit-spot generation proposed by Hirano et al. (2006).

At site B, three peridotite xenoliths (samples 2As, 2Al, and 2Aa) were found from a petit-spot volcano. Eruptions of a cluster of petit-spot volcanoes at site B are inferred to have occurred more recently than 1 Ma (Hirano et al., 2006) (Fig. 1(c)). Side-scan sonar data show the occurrence of another petit-spot volcano ca. 1 km southwest of 6K#878 (Hirano et al., 2006).

About a dozen ultramafic xenolith samples are included in the petit-spot alkaline basalt, but are mostly smaller than 1 cm in diameter. The xenoliths reported in this paper are relatively large xenoliths and are spinel lherzolites except samples 2Aa and 2A. Samples 2Aa and 2A are, respectively, lherzolite and olivine orthopyroxenite. All the xenoliths show a porphyroclastic to equigranular texture. They are sufficiently large (>2 cm diameter) to support noble gas isotopic analyses. The constituent minerals of the xenoliths largely have around 1 mm diameter average size, though sample 2A has large orthopyroxenes

with >5 mm diameter. The rims of some olivine grains in samples 2As, 2Al, and 2Aa are replaced by serpentine. Fresh and clear olivine grains were separated from each sample.

Major element contents of constituent minerals of the mantle xenoliths are presented in Table 2. The Fo values ($[\text{Mg}/(\text{Mg} + \text{Fe}) \times 100]$ of olivine) are 89.8–92.7, which are slightly higher than that of typical mantle: about 90 (e.g., Takahashi, 1986; Arai, 1994). The Cr# $[\text{Cr}/(\text{Cr} + \text{Al}) \times 100]$ of spinel of the petit-spot ultramafic xenoliths varies from 8 to 38 (Abe et al., 2006). The only analyzable spinel in this paper in the sample 2D is also high compared to the primary mantle value of about 10 (Arai, 1994). Those values suggest that the xenoliths were derived from mantle sources that had been partially melted. Generation of MORB could be considered as a possible depletion event of suboceanic mantle. Equilibrium temperatures were estimated based on Wells (1977) two-pyroxene geothermometer. The equilibrium temperatures of samples 2Aa and 2A are intermediate of those of the present xenoliths, which implies that samples 2Aa and 2A are also derived from a mantle source in a spinel-stability field. The pressure of the spinel-to-garnet transition is a function of the fertility of the peridotite. Peridotites with Mg# of 89.8–92.7 for olivine, as observed in the present xenoliths (Table 2), have transition pressure of 13–16 kb at 800–1100 °C (e.g. O'Neill, 1981), corresponding to a depth of 40–50 km below the sea bottom. The depth of the Gutenberg discontinuity, which is regarded as the boundary between the lithosphere and the asthenosphere, is around 80 km from the sea bottom in the northwestern Pacific (Shimamura and Asada, 1984; Kawakatsu et al., 2009). Therefore, the present xenoliths are believed to be samples derived from the old SOLM.

Presnall et al. (2002) proposed a model for the generation of MORB based on phase relations that MORB is a mixture of a small fraction of carbonatite melt generated at pressures of ca. 2.6–7 GPa and basaltic melt generated at ca. 0.9–1.5 GPa. Hirth and Kohlstedt (1996) reported that the extraction of water from olivine during the MORB melting process engenders a discontinuity of mantle viscosity resulting in formation of boundary between the lithosphere and the asthenosphere. Karato and Jung (1998) reinforced the model based on seismic properties of olivine suggesting that the depth of the Gutenberg discontinuity corresponds to the depth at which seismic wave attenuation changes because of different water contents. The

Table 2
Average compositions (wt.%) of minerals in suboceanic mantle xenoliths.

Dredge no.	6K#878				6K#878				6K#878			6K#880				6K#880				
	Samples				2As				2Al			2Aa				2D			2A	
Rocktype	Spinel-lherzolite xenolith				Spinel-lherzolite xenolith				Lherzolite xenolith			Spinel-lherzolite xenolith				Olivine orthopyroxenite				
Mineral	olivine	opx	cpx	spinel	olivine	opx	cpx	spinel	olivine	opx	cpx	olivine	opx	cpx	spinel	olivine	opx	cpx		
Mode (%)	56.9	25.5	16.5	0.2	68.1	18.7	12.1	0.5	66.1	20.0	14.0	65.7	25.7	5.0	3.6	22.3	73.4	4.3		
Mg#	92.75	91.86	92.41		90.94	90.19	91.99		89.75	90.09	94.11	90.73	91.61	91.02	73.56	90.64	90.40	93.78		
Cr#															21.15					
SiO ₂	42.07	56.96	54.16		41.44	55.48	53.17		41.35	55.79	54.19	41.23	56.10	53.67	0.22	41.08	55.02	53.03		
TiO ₂	0.02	0.09	0.21		0.00	0.10	0.50		0.02	0.09	0.46	0.02	0.13	0.26	0.94	0.01	0.14	0.43		
Al ₂ O ₃	0.02	2.20	3.07		0.00	4.60	6.07		0.00	4.89	6.28	0.05	3.27	4.02	46.86	0.01	4.96	3.63		
Cr ₂ O ₃	0.01	0.47	1.14		0.00	0.31	0.64		0.01	0.35	0.55	0.06	0.85	1.65	18.66	0.01	0.36	0.96		
FeO	7.03	5.38	2.45		8.77	6.32	2.22		9.83	6.28	1.73	8.93	5.35	3.04	12.82	9.07	6.16	2.06		
MnO	0.10	0.13	0.08		0.13	0.14	0.08		0.12	0.14	0.08	0.12	0.12	0.10	0.20	0.12	0.14	0.08		
MgO	50.45	34.02	16.77		49.36	32.63	14.28		48.29	32.06	15.53	49.10	32.81	17.25	20.00	49.31	32.58	17.39		
CaO	0.03	0.59	20.87		0.01	0.30	21.30		0.01	0.28	19.34	0.11	1.12	18.72	0.00	0.03	0.45	22.01		
Na ₂ O	0.02	0.06	1.18		0.00	0.03	1.71		0.01	0.03	1.78	0.01	0.12	1.16	0.00	0.01	0.08	0.36		
K ₂ O	0.02	0.02	0.02		0.01	0.02	0.01		0.02	0.02	0.02	0.01	0.01	0.01	0.00	0.02	0.02	0.02		
NiO	0.24	0.08	0.04		0.29	0.07	0.03		0.33	0.06	0.03	0.36	0.11	0.06	0.31	0.34	0.08	0.04		
Total	100.00	100.00	100.00		100.00	100.00	100.00		100.00	100.00	100.00	100.00	100.00	100.00	100.00	100.00	100.00	100.00		
T [°C]	989	±44			846	±88			1032	±57		1129	±31			1035	±81			

Multiple points in the core of a single grain of each mineral species were analyzed. Compositions of spinels in samples 2As and 2Al were not listed because the cation stoichiometry did not correspond to that of spinel, which result from oxidation of Fe and Cr during weathering. Equilibrium temperature (*T*) was estimated by two-pyroxene geothermometer of Wells (1977). opx, orthopyroxene; cpx, clinopyroxene. Major element compositions were analyzed using an electron probe microanalyzer (JEOL JXA-8800 at Tokyo Institute of Technology). The analyses were carried out using an accelerating voltage of 20 kV and a beam current of 20 nA. Integrated times for measurements were 100 s for most elements and 20 s for Na and K. We analyzed the model mineralogy by a model analysis method using image processing proposed by Nishimoto (1996).

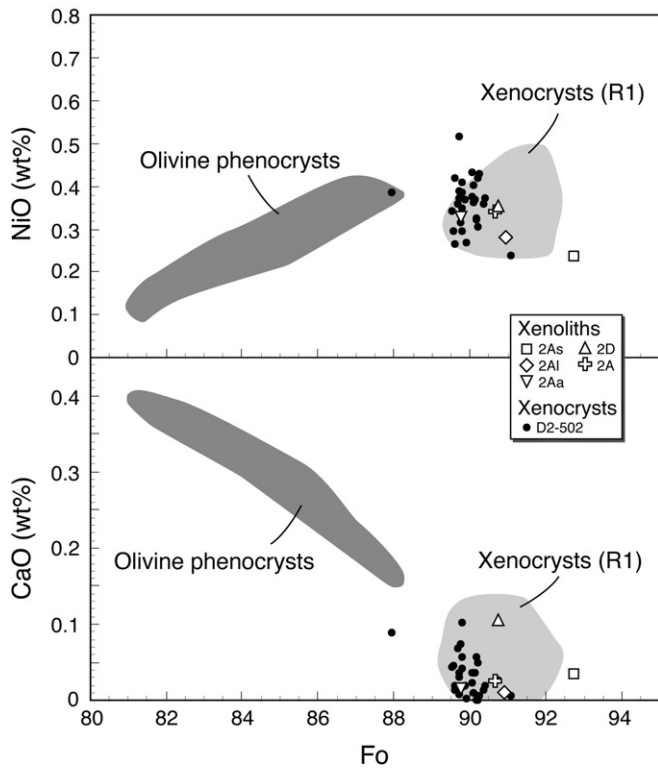


Fig. 2. Contents of NiO and CaO, and Fo values of large olivine megacrysts (D2-502) and olivines from xenolith samples. Shaded areas colored in pale gray and dark gray, respectively, represent compositions of xenocrystic olivines (sample R1) and olivine phenocrysts selected from a rock that included the sample R1 (Hirano et al., 2004).

depth of the Gutenberg discontinuity in the oceanic upper mantle is around 60–80 km and is independent of age (Karato and Jung, 1998). These facts indicate that the boundary between the lithosphere and the asthenosphere in the oceanic mantle was established by extraction of water from fertile asthenospheric mantle during generation of the MORB magma. Subsequently, the resulting compositional layering has been retained by the viscosity discontinuity (Gaherty et al., 1999). Consequently, the mantle sources of the present xenoliths are possibly a part of the depleted residue left after MORB extraction.

Two compositionally distinct olivines exist in the petit-spot lava blocks; large olivine megacrysts with a reaction rim and small olivine phenocrysts (Hirano et al., 2004). The average sizes of the large olivine megacrysts and the small olivine phenocrysts are, respectively, about

2 mm and less than 0.2 mm in diameter. Hirano et al. (2004) reported that the small olivine phenocrysts have major element compositions in equilibrium with the host basalt while major element compositions of the large olivine megacrysts resemble those of typical mantle peridotites. Similarly, we measured major element compositions of the large olivine megacrysts. Fig. 2 shows NiO, MnO and Fo values of the large olivine megacrysts (D2-502a and D2-502b) and olivines from the xenoliths along with the data of both xenocrystic olivines (R1) and olivine phenocrysts reported by Hirano et al. (2004). Results show that the large olivine megacrysts have Fo values of about 90, which are within the range of those of the xenoliths. In addition, contents of CaO and NiO of the large olivine megacrysts respectively show no appreciable difference from those of the xenoliths. These facts suggest that the large olivine megacrysts are xenocrysts derived from the upper mantle. Xenocrysts (D2-502a and D2-502b) in lava blocks were separated from small olivine phenocrysts using a sieve.

The xenoliths and the xenocrysts include fluid and melt inclusions. The fluid inclusions have a negative crystal shape, a type of inclusion reflecting the crystal form of a host mineral. The fluid inclusions are usually less than 10 μm in diameter. Based on micro-Raman spectroscopic analyses, CO₂ was identified in the fluid inclusions. The melt inclusions have a dendritic and vermicular shape. They often coexist with CO₂ fluid.

2.1. Analytical method of noble gases

Grains were soaked in 2 N HNO₃ for half an hour at 70 °C. Subsequently, they were washed ultrasonically in distilled water, ethanol, and acetone. Noble gases were extracted from olivine grains through in-vacuo crushing. Before crushing, the crushing vessels were preheated to 150 °C overnight to reduce blank levels. Noble gas analyses were performed using a sector-type mass spectrometer (VG-5400) installed at JAMSTEC. Sensitivities and isotopic ratios of noble gases were calibrated using a diluted air standard and Kaminoyama well gas with ³He/⁴He of 5.68 Ra (Hanyu et al., 2007). Uncertainty for all noble gas abundances is less than 5% at 1 σ. More detailed analytical conditions for noble gases at JAMSTEC have been reported elsewhere (Hanyu et al., 2007).

3. Results

Results of noble gas isotope measurements are presented in Table 3 along with noble gas data of xenocrystic olivines (sample R1) reported by Yamamoto et al. (2003). In this study we do not discuss noble gas abundances extracted using the crushing method, which cannot be taken as a reliable index to characterize the present samples because the abundances depend on numerous factors such as a crushing efficiency, number and size of fluid inclusions, existence of shrinkage bubble in melt inclusions, and size of mineral grains. Fig. 3 shows the

Table 3
Noble gas isotopic compositions of olivines from suboceanic mantle xenoliths and xenocrystic olivines.

Samples	Weight g	⁴ He (10 ⁻⁸)	²⁰ Ne (10 ⁻¹²)	⁴⁰ Ar (10 ⁻⁸)	⁸⁴ Kr (10 ⁻¹²)	¹³⁰ Xe (10 ⁻¹²)	³ He/ ⁴ He (Ra)	²⁰ Ne/ ²² Ne	²¹ Ne/ ²² Ne	⁴⁰ Ar/ ³⁶ Ar	⁴ He/ ²¹ Ne*	⁴ He/ ⁴⁰ Ar*
<i>Xenoliths</i>												
2As	0.456	0.23	39	4.7	2.5	0.021	8.46 ± 0.86	*	*	347 ± 3		0.33
2Al	0.678	0.15	23	2.2	1.2	0.012	8.23 ± 0.53	*	*	462 ± 6		0.181
2D	0.699	19	138	240	8.9	0.082	7.03 ± 0.39	9.87 ± 0.04	0.0310 ± 0.0005	6642 ± 774	6.8E+06	0.085
<i>Xenocrysts</i>												
D2-502a	0.648	1.4	17	23	1.2	0.014	7.42 ± 0.43	9.90 ± 0.07	0.0329 ± 0.0014	5922 ± 384	2.0E+06	0.06
D2-502b	1.327	9.6	50	100	5.3	0.041	7.11 ± 0.40	10.05 ± 0.06	0.0324 ± 0.0006	3776 ± 132	5.7E+06	0.10
<i>Xenocrysts (after Yamamoto et al. (2003))</i>												
R1 (crushing)	0.245	76	120	24	5.4	0.060	7.20 ± 0.31	9.70 ± 0.30	0.0306 ± 0.0040	1647 ± 30	3.8E+07	3.9
R1 (heating)	1.384	141	338	71	24	0.31	7.30 ± 0.12	9.73 ± 0.23	0.0294 ± 0.0020	732 ± 10		5.7

N.B., unit for abundance is cm³ STP/g. *: not measured. ⁴⁰Ar* is ⁴⁰Ar corrected for atmospheric contamination.

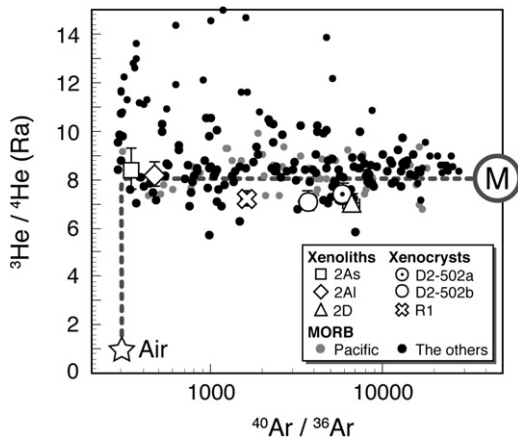


Fig. 3. $^3\text{He}/^4\text{He}$ and $^{40}\text{Ar}/^{36}\text{Ar}$ diagram of the samples and MORB. Error bars for the samples represent 1σ uncertainties. The broken line represents a mixing line between air and MORB source (M). Data sources of MORB are Pacific MORB (Kyser and Rison, 1982; Ozima and Podosek, 1983; Ozima and Zashu, 1983; Allègre et al., 1983; Marty and Ozima, 1986; Sarda et al., 1988; Marty, 1989; Hiyagon et al., 1992; Niedermann et al., 1997; Niedermann and Bach, 1998; Stronck et al., 2008) and other MORB (Kyser and Rison, 1982; Allègre et al., 1983; Jambon et al., 1985; Marty and Ozima, 1986; Staudacher et al., 1989; Hiyagon et al., 1992; Moreira et al., 1995, 1996, 1998; Battani, 1996; Kumagai and Kaneoka, 1998, 2003, 2005; Sarda et al., 2000; Moreira and Allègre, 2002; Macpherson et al., 2005).

$^3\text{He}/^4\text{He}$ versus $^{40}\text{Ar}/^{36}\text{Ar}$ of the samples and MORB. Helium isotopic ratios of the present samples are 7.0–8.5 Ra, which are within the range of MORB values (8.75 ± 2.14 Ra; Graham, 2002), but some samples show $^3\text{He}/^4\text{He}$ that are slightly lower than the average value of Pacific MORB (8.13 ± 0.98 Ra; Graham, 2002). Argon isotopic ratios of samples 2As and 2AI, whose olivines have been partly replaced by serpentine, are less than 500, but are high compared to that of air (295.5). Ratios of $^{40}\text{Ar}/^{36}\text{Ar}$ of up to 10,000 observed in other samples are common for MORB (Fig. 3). Fig. 4 depicts the neon isotopic data on the three-isotope diagram along with MORB data. Although the neon isotopic compositions of the samples have a large atmospheric contribution, some samples show values that are distinguishable from atmospheric neon beyond experimental uncertainty. In fact, MORB has a linear correlation, as depicted in Fig. 4, which is regarded as a mixing line between a MORB source and atmospheric component (Sarda et al. 1988). The samples are shown as near the mixing line.

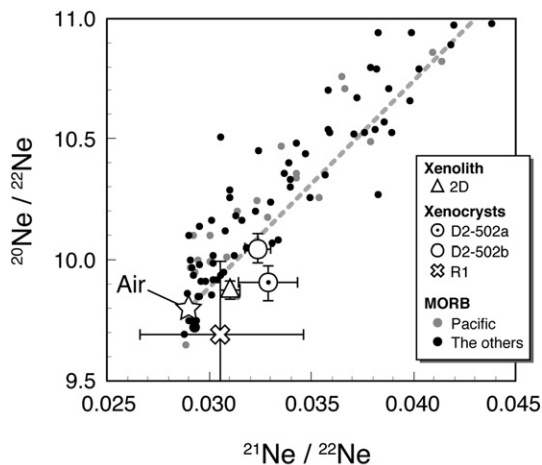


Fig. 4. A Ne three-isotope diagram of the samples and MORB. Error bars for the samples represent 1σ uncertainties. MORB data with $^3\text{He}/^4\text{He}$ of more than 10 Ra are not shown. The broken line represents a mixing line between the air and MORB source. Most MORB data are from Fig. 2. The Ne data of Craig and Lupton (1976), Sarda et al. (1988) and Marty (1989) are added to the other MORB. There is little difference between Pacific MORB and the other MORB.

Slightly low $^{20}\text{Ne}/^{22}\text{Ne}$ of the samples at a given $^{21}\text{Ne}/^{22}\text{Ne}$ compared to MORB might result from the accumulation of nucleogenic ^{21}Ne that was generated in-situ in the Pacific Plate. Overall, no significant difference was found in noble gas isotopic compositions between the samples and MORB. Isotopic compositions of Kr and Xe were not measured because of their low concentrations.

The samples except sample R1 have low $^4\text{He}/^{40}\text{Ar}^*$ (0.06–0.33) compared to the MORB value (4.7 ± 1.6 ; Burnard, 2001). An accumulated $^4\text{He}/^{40}\text{Ar}^*$ production ratio in the upper-mantle source with a K/U ratio of $19,000 \pm 2600$ by mass (Arevalo et al., 2009) is 1.0–1.3 for time scales of 4.6 billion years. The instantaneous production ratio of $^4\text{He}/^{40}\text{Ar}^*$ in the mantle source is 2.7–3.6, but $^4\text{He}/^{40}\text{Ar}^*$ ratios of the present samples are much lower than the production ratio (1.0–3.6).

The $^4\text{He}/^{21}\text{Ne}^*$ is a useful index to examine the cause of the low $^4\text{He}/^{40}\text{Ar}^*$, where $^{21}\text{Ne}^*$ denotes $^{21}\text{Ne}^*$ corrected for atmospheric contributions (defined as $^{21}\text{Ne}^* = ^{21}\text{Ne}_{\text{sample}} \times [(^{21}\text{Ne}/^{22}\text{Ne})_{\text{sample}} - (^{21}\text{Ne}/^{22}\text{Ne})_{\text{air}}]$), although it is difficult to calculate $^{21}\text{Ne}^*$ accurately for data with a Ne isotopic composition that resembles that of air, as observed in this study. Fig. 5 presents a diagram of $^4\text{He}/^{21}\text{Ne}^*$ and $^4\text{He}/^{40}\text{Ar}^*$ for the samples along with data of SCLM. The shaded area represents a mass fractionation trend starting from the mantle production ratios. Clearly, $^4\text{He}/^{21}\text{Ne}^*$ of SCLM is correlated with $^4\text{He}/^{40}\text{Ar}^*$. The positive correlation of SCLM can be regarded as a significant and systematic elemental fractionation of ^4He from $^{21}\text{Ne}^*$ and $^{40}\text{Ar}^*$ (Patterson et al., 1994; Honda and Patterson, 1999; Yamamoto et al., 2009a). The samples plot off the correlation of SCLM. This might be attributed to a possible difference in $^4\text{He}/^{40}\text{Ar}^*$ of a starting mantle source in addition to the uncertainty of $^{21}\text{Ne}^*$. Slightly low K/U has been reported for SCLM (2000–12,000; Wakita et al., 1967), which implies a high production ratio of $^4\text{He}/^{40}\text{Ar}^*$ of >3 . On the other hand, MORB sources have $^4\text{He}/^{40}\text{Ar}^*$ of 1.0–3.6, as described above. Therefore, low $^4\text{He}/^{40}\text{Ar}^*$ of the samples at a given $^4\text{He}/^{21}\text{Ne}^*$ results from the elemental fractionation of a mantle source, which originally has a MORB source like $^4\text{He}/^{40}\text{Ar}^*$.

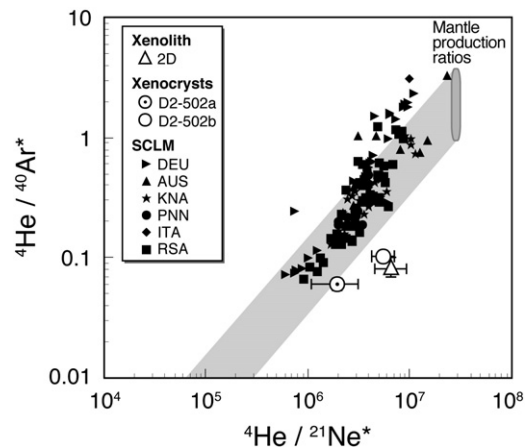


Fig. 5. $^4\text{He}/^{21}\text{Ne}^*$ and $^4\text{He}/^{40}\text{Ar}^*$ diagram of the samples and SCLM with crushing experiments, where asterisks denote correction for atmospheric contribution. Error bars for the samples represent 1σ uncertainties. Sample R1 is not shown because of the extremely high uncertainty of $^4\text{He}/^{21}\text{Ne}^*$ ($>200\%$). Data sources of SCLM are as follows: peridotite xenoliths from Germany (DEU) (Gautheron et al., 2005; Buikin et al., 2005), Australia (AUS) (Matsumoto et al., 2000), Kenya (KNA) (Hopp et al., 2007a), Pannonian (PNN) (Buikin et al., 2005), and Red Sea (RSA) (Hopp et al., 2004, 2007b); orogenic peridotites from Italy (ITA) (Matsumoto et al., 2005). Data with $^{21}\text{Ne}/^{22}\text{Ne}$ and $^{40}\text{Ar}/^{36}\text{Ar}$ of less than 0.03 and 320, respectively, are not shown. The $^4\text{He}/^{21}\text{Ne}^*$ production ratio in the mantle is estimated as 2.78×10^7 (Yatsevich and Honda, 1997; Leya and Wieler, 1999) because ^{21}Ne can be generated nucleogenically from (α, n) reaction on ^{18}O and (n, α) reaction on ^{24}Mg (Wetherill, 1954). The $^4\text{He}/^{21}\text{Ne}^*$ production ratio in the lithosphere is determined primarily by its chemical composition, which is unlikely to vary dramatically among reservoirs. Therefore, the $^4\text{He}/^{21}\text{Ne}^*$ of the mantle is likely to be constant. Regarding $^4\text{He}/^{40}\text{Ar}^*$, the possible difference in K/U between the SCLM and the SOLM engenders diversity of $^4\text{He}/^{40}\text{Ar}^*$ in the mantle.

4. Discussion

Overall noble gas isotopic compositions of the samples resemble those of MORB, implying that the MORB-source mantle has a wide distribution in the SOLM. It raises an interesting question of how the old SOLM avoids radiogenic change in $^3\text{He}/^4\text{He}$. The samples show low $^4\text{He}/^{21}\text{Ne}^*$ and $^4\text{He}/^{40}\text{Ar}^*$. The other question is how and when depletion in lighter noble gases occurred in the old SOLM.

4.1. MORB-like $^3\text{He}/^4\text{He}$ in the old SOLM

The MORB-like $^3\text{He}/^4\text{He}$ of the samples is an interesting finding. The samples are derived from the Early Cretaceous Pacific Plate. Such an old plate is expected to accumulate radiogenic nuclides. Herein we shall outline the change in $^3\text{He}/^4\text{He}$ over time. Fig. 6(a) shows the He isotopic ratio as functions of timescale and $^3\text{He}/\text{U}$ ratio. Typically, mantle peridotites have U contents of 10–50 ppb (Yamamoto et al., 2009b). Adopting total ^3He content of sample R1 obtained using heating method (1.4×10^{-11} ccSTP/g), the $^3\text{He}/\text{U}$ molar ratio of a mantle source is 5×10^{-6} (1.4×10^{-11} ccSTP/g ^3He and 30 ppb U); then $^3\text{He}/^4\text{He}$ decreases from 8.75 to 5.1 Ra over 135 million years. The samples described herein do not show such low $^3\text{He}/^4\text{He}$. The reason for the use of ^3He content of sample R1 for the above estimation is described briefly here; details are discussed later (see 4.2.). Low $^4\text{He}/^{40}\text{Ar}^*$ ratios of some samples were regarded as consequences of the diffusive loss of helium by recent magmatism in this region. Consequently, we cannot use the samples with $^4\text{He}/^{40}\text{Ar}^*$ lower than the theoretical production ratio of $^4\text{He}/^{40}\text{Ar}^*$. They are inappropriate as a reference of the SOLM. The ^3He content extracted by heating of sample R1 is the only suitable data for use in estimation.

Two possibilities exist to reconcile this contradiction. One possibility is the influx of a component with MORB-like $^3\text{He}/^4\text{He}$ from the asthenosphere via diffusion or infiltration of a noble gas-

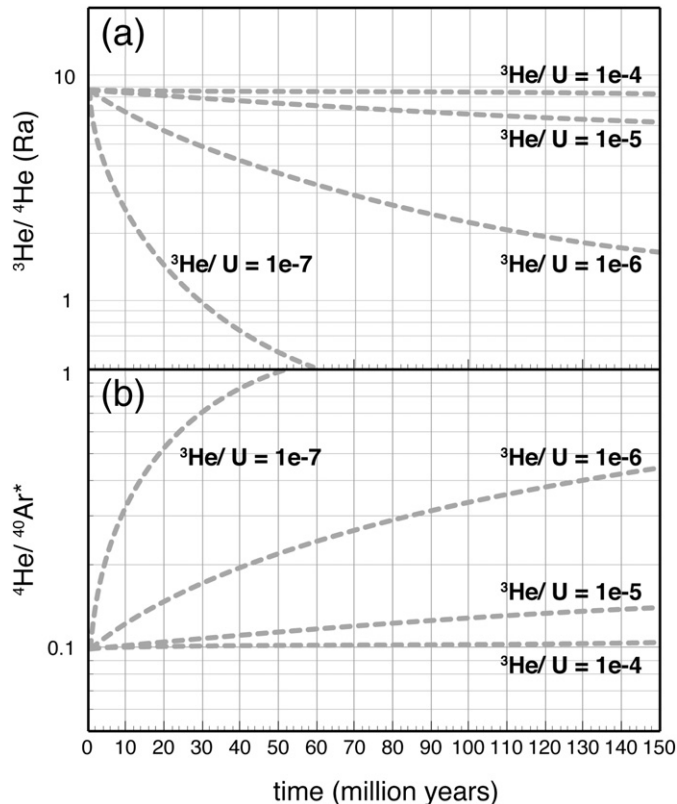


Fig. 6. Radiogenic change of (a) $^3\text{He}/^4\text{He}$ and (b) $^4\text{He}/^{40}\text{Ar}^*$ as a function of $^3\text{He}/\text{U}$ molar ratio. Calculations are based on the original mantle source with K/U of 19,000 by mass (Arevalo et al., 2009) and Th/U of 3.1 by mass (Staudacher et al., 1989).

bearing fluid or melt. Theoretical thermal models of the oceanic lithosphere show that spinel-lherzolite phase in the 135-million-year-old oceanic lithosphere has a temperature of less than 900 °C (Stein and Stein, 1992; Doin and Fleitout, 1996). Even at 1200 °C, the diffusion coefficient of ^3He is 1.9×10^{-10} cm²/s (Trull and Kurz, 1993), corresponding to average diffusion distance of 9 m for 135 million years. The distance is too small to change He isotopic compositions of the lithosphere. The assumption that the SOLM traps fluid or melt derived from the asthenosphere with MORB-like noble gas isotopic compositions remains convincing. Moreira and Sarda (2000) proposed the possibility that, in the early stage of degassing of ocean island magma, the distillation process generates small vesicles with low $^4\text{He}/^{40}\text{Ar}^*$; the SOLM might trap such early evolved vesicles during magma percolation. Although a similar concept—that the SOLM traps early evolved vesicles generated in the asthenosphere-derived magma—seems to explain the MORB-like $^3\text{He}/^4\text{He}$ and low $^4\text{He}/^{40}\text{Ar}^*$ of the samples plausibly, it is not yet satisfactorily applicable to the samples, whose equilibrium temperatures suggest that the samples were derived from various depths in the SOLM.

Another possibility is that the SOLM was isolated after its formation by MORB extraction with high He/U ratio resulting from MORB generation. A recent experimental study of He partitioning in mantle minerals has demonstrated that partial melting of the mantle engenders a residual mantle source with high He/U ratio (Parman et al., 2005). Herein we estimate the $^3\text{He}/\text{U}$ ratio of MORB source as follows. The ^3He content of predegassed MORB can be estimated as $3.1 \pm 1.4 \times 10^{-10}$ ccSTP/g using $\text{CO}_2/^3\text{He}$ molar ratio of $2.1 \pm 0.6 \times 10^9$ (Resing et al., 2004) and CO_2 content of 0.14 ± 0.05 wt.% (Holloway, 1998). The U content of MORB is estimated as 54 ± 14 ppb (Arevalo et al., 2009). Then $^3\text{He}/\text{U}$ molar ratio of MORB is $6.1 \pm 3.2 \times 10^{-5}$, which reflects the $^3\text{He}/\text{U}$ ratio of the MORB source because both ^3He and U are highly incompatible elements in the mantle. A $^3\text{He}/\text{U}$ molar ratio of 1.6×10^{-5} is necessary to explain the slightly low $^3\text{He}/^4\text{He}$ (7.0 Ra) of sample 2D by radiogenic accumulation of ^4He over 135 million years in a mantle source, which initially had MORB-like $^3\text{He}/^4\text{He}$ (8.75 Ra). The $^3\text{He}/\text{U}$ (1.6×10^{-5}) is comparable to that of the MORB source ($6.1 \pm 3.2 \times 10^{-5}$). The similarity is expected to corroborate the experimental data of He–U partitioning into olivine proposed by Parman et al. (2005), although there is no assurance of applicability of this assumption to the deeper mantle.

4.2. Non-radiogenic $^4\text{He}/^{40}\text{Ar}^*$ of the old SOLM

These samples show $^4\text{He}/^{40}\text{Ar}^*$ lower than the production ratio in the mantle. Low $^4\text{He}/^{40}\text{Ar}^*$ is frequently reported for SCLM xenoliths and is correlated well with $^4\text{He}/^{21}\text{Ne}^*$, as portrayed in Fig. 5. Although possible high K/U of the mantle source results in low $^4\text{He}/^{40}\text{Ar}^*$, the correlation in SCLM eliminates the possibility. Alternatively, a depletion event in the mantle is considered as the probable cause of the low $^4\text{He}/^{40}\text{Ar}^*$ and $^4\text{He}/^{21}\text{Ne}^*$. SCLM data would give a hint about the cause of the depletion event. The low $^4\text{He}/^{40}\text{Ar}^*$ of SCLM is reported only from mantle xenoliths. All orogenic peridotites have $^4\text{He}/^{40}\text{Ar}^*$ of >1 . For example, $^4\text{He}/^{40}\text{Ar}^*$ of orogenic peridotites in Finero (Matsumoto et al., 2005) and Horoman (Matsumoto et al., 2001) are, respectively, 3.1–47.5 and 1.5–5.1. Song et al. (2009) reported $^4\text{He}/^{40}\text{Ar}^*$ of 0.9 and 2.6 from orogenic harzburgites in Northwest China. In addition, Kumagai et al. (2003) reported $^4\text{He}/^{40}\text{Ar}^*$ of 1.7 and 8.5 from dredged abyssal peridotites. These facts suggest that the low $^4\text{He}/^{40}\text{Ar}^*$ of SCLM xenoliths are related to magmatic activity. Furthermore, variation of $^4\text{He}/^{40}\text{Ar}^*$ among sample localities implies that the phenomenon is not caused by host magma entraining the mantle xenoliths to the Earth's surface, suggesting instead that the depletion is related to precursor magmatism before eruption of the host magma of the xenoliths. The precursor magmatism is explained in greater detail later in this paper. Here we particularly examine the magmatic depletion mechanism.

Matsuda and Marty (1995) and Burnard (2004) proposed a model to represent kinetic fractionation of He/Ar in magma during mantle melting. When magma infiltrates into the mantle or is generated in the mantle, noble gases in the mantle are partitioned into magma. The high diffusivity of He is responsible for low $^4\text{He}/^{40}\text{Ar}$ in residual mantle if movement of the noble gases in the mantle is governed by a vacancy diffusion mechanism. The SOLM experienced large-scale melting during MORB generation. The MORB generation is not, however, a cause of the low $^4\text{He}/^{40}\text{Ar}^*$ in the present samples because ancient fractionation of $^4\text{He}/^{40}\text{Ar}^*$ engenders subsequent radiogenic ingrowth of $^3\text{He}/^4\text{He}$ and $^4\text{He}/^{40}\text{Ar}^*$ over time. We calculate the radiogenic ingrowth in the fractionated mantle source. During production of one order of magnitude lower $^4\text{He}/^{40}\text{Ar}^*$ in a mantle source by diffusive fractionation, the ^3He content drops to around 2% (Yamamoto et al., 2009a). Consequently, the $^3\text{He}/\text{U}$ ratio of the mantle source also decreases to around 2%, i.e., MORB-like $^3\text{He}/\text{U}$ ($6.1 \pm 3.2 \times 10^{-5}$ by mol) will be decreased to ca. 1×10^{-6} by mol. Fig. 6 shows that radiogenic ^4He and ^{40}Ar in the fractionated mantle induces rapid changes in $^3\text{He}/^4\text{He}$ and $^4\text{He}/^{40}\text{Ar}^*$. The $^3\text{He}/^4\text{He}$ of the fractionated mantle source will change radiogenically from 8.75 to 1.9 Ra for 135 million years. Consequently, MORB-like $^3\text{He}/^4\text{He}$ of the samples shows that the low $^4\text{He}/^{40}\text{Ar}^*$ in the old SOLM is not caused by the MORB generation but by a recent kinetic fractionation.

Yamamoto et al. (2009a) calculated the diffusive change in $^4\text{He}/^{40}\text{Ar}$ and $^3\text{He}/^4\text{He}$ based on the diffusive fractionation model proposed by Matsuda and Marty (1995) and Burnard (2004). Similarly, we calculated a diffusive fractionation trend starting from a mantle source (shaded area in Fig. 7). In the calculation, we consider the diffusion of noble gases in a mantle source bounded by two parallel planar magma channels, which is not saturated with noble gases. Infiltration of magma engenders the progressive removal of noble gases from the mantle source to the magma channels if noble gases are initially distributed homogeneously throughout the mantle source. The shaded area in Fig. 7 depicts averaged noble gas isotopic compositions of the mantle source. The present data support the trend.

Diffusive fractionation will occur in phenocrysts in ascending magma (Harrison et al., 2004; Nuccio et al., 2008; Yamamoto et al.,

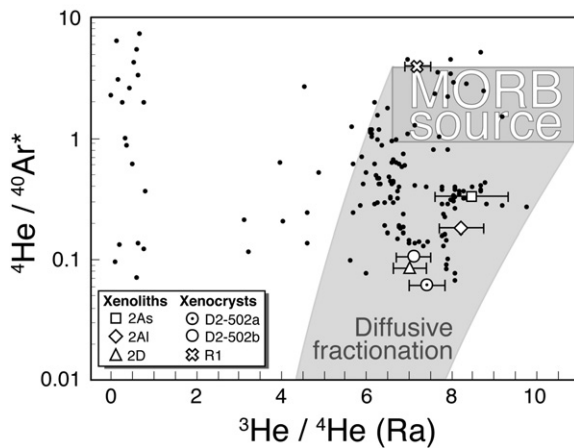


Fig. 7. $^3\text{He}/^4\text{He}$ versus $^4\text{He}/^{40}\text{Ar}^*$ diagram for the present mantle-derived xenoliths and xenocrysts with data for SCLM-derived peridotites with crushing experiments, as indicated by dots. MOST SCLM data are from Fig. 5. The data of Yamamoto et al. (2004), Kim et al. (2005), Czuppon et al. (2009) and Song et al. (2009) are added to the SCLM. The shaded area represents a trend of diffusive fractionation from the MORB source (gray rectangle) using the elemental diffusivity ratio of He and Ar ($D_{\text{He}}/D_{\text{Ar}}$) equal to 3.16 and the isotopic diffusivity ratio of ^3He and ^4He ($D_{^3\text{He}}/D_{^4\text{He}}$) equal to 1.05. The low isotopic diffusivity ratio is plausible. Values lower than the theoretical value of 1.15 were obtained from several materials such as basalt glass (Trull and Kurz, 1999), quartz (Shuster and Farley, 2005), and olivine and pyroxene (Trull and Kurz, 1993). The $^3\text{He}/^4\text{He}$ and $^4\text{He}/^{40}\text{Ar}^*$ of the MORB source are, respectively, 8.75 ± 2.14 (Graham, 2002) and 1.0–3.6 (see the text). Error bars for $^4\text{He}/^{40}\text{Ar}^*$ are smaller than the size of each symbol (less than 10%).

2009a). The present xenocrysts would be almost free from diffusive fractionation after trapping by host magma because, considering the migration rate for alkali magma (tens of centimeters per second (Spera, 1984; Milashev, 1988; Peslier and Luhr, 2006) to several meters per second (Demouchy et al., 2006)), the host magma erupts within a week after trapping of xenoliths, even from 60 km depth. In contrast, it takes six months to reduce $^4\text{He}/^{40}\text{Ar}^*$ of olivine grain with 1 mm diameter from 3 to 0.1 at 1200 °C (Yamamoto et al., 2009a), which implies that diffusive fractionation in phenocrysts mostly occurs within the magma chamber or during the post-eruption cooling stage. Petit-spot volcanoes are small knolls on the ocean floor. We therefore cannot expect the presence of a massive magma chamber beneath the volcanoes (Fujiwara et al., 2006, 2007). Furthermore, when the magma emerged to ocean floor, the diffusive fractionation in the xenocrysts was suspended by lava quenching. Therefore, the low $^4\text{He}/^{40}\text{Ar}^*$ of the present samples necessarily means that diffusive fractionation occurs in mantle sources.

Diffusively fractionated mantle is expected to have a lower He/U ratio. Assuming a fractionated mantle source with a $^3\text{He}/\text{U}$ molar ratio of 1×10^{-6} as estimated above, Fig. 6 shows that $^3\text{He}/^4\text{He}$ changes from 8.75 to 6.9 Ra for 10 million years. Furthermore, $^3\text{He}/^4\text{He}$ is decreased respectively to 5.7 and 4.8 Ra over 20 and 30 million years. Therefore, the MORB-like $^3\text{He}/^4\text{He}$ of the present samples implies that the depletion event occurred within 10 million years before the present xenoliths and that xenocrysts were entrained by host magma and emplaced on the ocean floor. The origin of the precursor volcanism is discussed in the following section.

Although radiogenic nuclides have been accumulated in the xenoliths and the xenocrysts after eruption, the post-eruptive radiogenic addition has a negligible effect on noble gas isotopic compositions of fluid or melt inclusions (e.g., Kurz, 1986; Graham et al., 1992a,b).

4.3. Long-term activity of petit-spot volcanism

The diffusive fractionation caused by infiltration of magma depends on the diffusion coefficient, timescale and channel spacing. The mantle xenoliths have sizes of more than 2 cm diameter. Even if a mantle source is infiltrated by magma channels with channel spacing of 2 cm, it takes around 400 years to change $^4\text{He}/^{40}\text{Ar}^*$ from 3 to 0.1 at 1200 °C (Fig. 8). The host magma entraining the mantle xenoliths is not responsible for the depletion process as recorded in the samples. Consequently, low $^4\text{He}/^{40}\text{Ar}^*$ ratios of the samples indicate that the other recent magmatism existed before the host magma of the samples erupted. In this region, no recent magmatism other than the petit-spot volcanism was found: the precursor magma is expected to be a part of the petit-spot

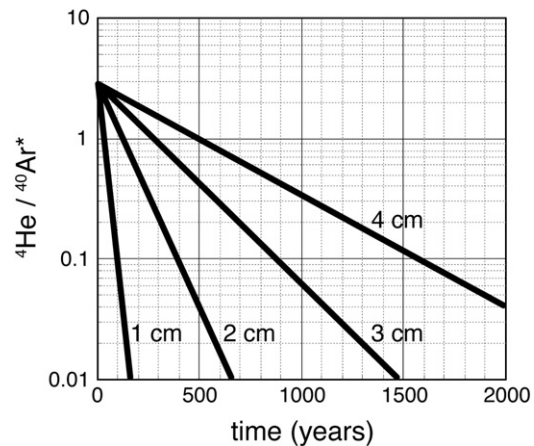


Fig. 8. Averaged $^4\text{He}/^{40}\text{Ar}^*$ in a mantle source bounded by two parallel planar magma channels as functions of time and channel spacing at 1200 °C. The lines are labeled, with numbers showing the channel spacing. We calculated $^4\text{He}/^{40}\text{Ar}^*$ following the diffusion equation represented by Yamamoto et al. (2009a).

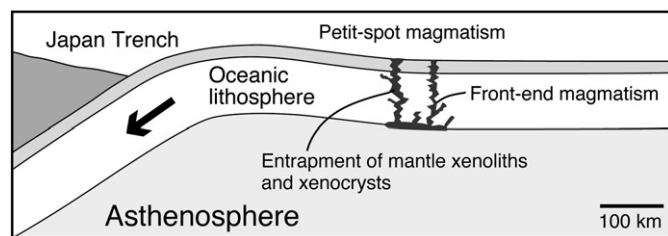


Fig. 9. Schematic cross-section around the present petit-spot volcanoes. Hirano et al. (2006) proposed that petit-spot magmatism originated from lithospheric fractures in response to plate flexure during subduction. The front-end magmatism preferentially extracts lighter noble gases such as He and Ne from the oceanic lithosphere. Consequently, xenoliths entrained by magmatism in later stages might have low $^4\text{He}/^{40}\text{Ar}^*$.

volcanism. Actually, some petit-spot volcanoes have multiple lava flows with different eruption ages (Hirano et al., 2008). The petit-spot volcanoes are expected to be polygenetic with a long active period.

Fig. 9 portrays a schematic cross-section around the Japan Trench to the outer rise. The earliest magma (front-end magmatism) can entrain xenoliths and xenocrysts from the unfractionated old SOLM. During front-end magmatism, He/Ar of the lithosphere around the magma channels will decrease with time. The xenoliths and the xenocrysts entrained by the magma in a later stage possibly have low $^4\text{He}/^{21}\text{Ne}^*$ and $^4\text{He}/^{40}\text{Ar}^*$. The eruption ages of the host magma in site A are noteworthy (Fig. 1(b)). The petit-spot volcano involving sample R1 probably erupted as front-end magmatism because it shows the oldest eruption age (6.0 ± 0.3 Ma) at the center of distribution of the petit-spot volcanoes at site A. For that reason, sample R1 shows no low He/Ar. The other samples in this region show low $^4\text{He}/^{40}\text{Ar}^*$.

Petit-spot volcanism is thought to be a common magmatic activity occurring near subducting plates resulting from subduction-related plate flexure (Hirano et al., 2001, 2004, 2006). Long-standing magmatic activity within the subducting plates carries the potential for a major control of several geological characteristics in subduction zone. For example, the depletion in volatile elements with high diffusivity in the subducting plate might be inherited to subduction-related fluid or melt. In addition, remaining heat in the subducting plate caused by the petit-spot volcanism substantially affects the thermal structure of both the mantle wedge and the subducting slab itself. Further investigation of peridotite xenoliths entrained by the petit-spot magma in later stages enables us to elucidate the potential of petit-spot volcanism for a subduction environment.

5. Summary

We analyzed noble gas isotopic compositions of three spinel-ilmenite xenoliths and two sets of xenocrystic olivines in three submarine volcanoes that are part of the petit-spot volcanoes, which erupted within several million years at the 135-million-year-old northwestern Pacific Plate. The xenoliths are representative of the subducting SOLM. Overall noble gas isotopic compositions resemble those of MORB, which indicates that the SOLM with noble gas compositions like MORB exists in this area, reflecting a more ubiquitous character of the MORB-source mantle overall. To maintain the MORB-like $^3\text{He}/^4\text{He}$ (>7.0 Ra) for 135 million years, the lithosphere is regarded to have a $^3\text{He}/\text{U}$ molar ratio of $>1.6 \times 10^{-5}$, which is comparable to that of MORB source ($6.1 \pm 3.2 \times 10^{-5}$ by mol). This ratio apparently indicates that MORB generation does not strongly affect the $^3\text{He}/\text{U}$ ratio of the upper mantle.

On the other hand, the present samples show $^3\text{He}/^4\text{He}$, low $^4\text{He}/^{21}\text{Ne}^*$ and $^4\text{He}/^{40}\text{Ar}^*$. Based on a model of diffusive fractionation in the mantle with the magma channel, the characteristics imply a recent depletion event in the mantle. No recent magmatic activity has taken place in this area other than the petit-spot volcanism: the depletion event must therefore be related to the petit-spot volcanism. Such volcanism over a

long active period can affect both the geochemical and geothermal structure of the subducting oceanic plates.

Acknowledgments

The editor and two anonymous reviewers provided very constructive comments. We are deeply appreciative of the cooperation of all crews, the marine technicians and the shipboard scientific parties of the JAMSTEC cruises (KR97-11, KR03-07, KR04-08 and YK05-06). We appreciate H. Kumagai and K. Sato for their help in analyzing noble gases. K. Nishimura provided valuable suggestions related to the diffusive fractionation model. The cruise YK05-06 was partly supported by Grant-in-Aid for Scientific Research (B) (1) (No. 17340136), Japan Society for the Promotion of Science (JSPS). This study was financially supported in part by Research Fellowships of the Japan Society for the Promotion of Science (JSPS) for Young Scientists and Research Abroad to J. Y.

References

- Abe, N., Yamamoto, J., Hirano, N., Arai, S., 2006. Petrology and geochemistry of mantle xenoliths from petit-spot volcano, NW Pacific Plate. *Geochim. Cosmochim. Acta* 70, A1.
- Allègre, C.J., Staudacher, T., Sarda, P., Kurz, M., 1983. Constraints on evolution of Earth's mantle from rare gas systematics. *Nature* 303, 762–766.
- Amante, C., Eakins, B.W., 2008. ETOPO1 1 Arc-Minute Global Relief Model. Procedures, Data Sources and Analysis, National Geophysical Data Center, NESDIS, NOAA, U.S. Department of Commerce, Boulder, CO, August 2008.
- Arai, S., 1994. Characterization of spinel peridotites by olivine-spinel compositional relationships: review and interpretation. *Chem. Geol.* 113, 191–204.
- Arevalo Jr., R., McDonough, W.F., Luong, M., 2009. The K/U ratio of the silicate Earth: insights into mantle composition, structure and thermal evolution. *Earth Planet. Sci. Lett.* 278, 361–369.
- Battani, A., 1996. Systematique des gaz rares dans les basalts de l'océan Indien. Rapports de stage Année 1995–1996. Université Paris 7 Denis Diderot.
- Buikin, A., Trieloff, M., Hopp, J., Althaus, T., Korochantseva, E., Schwarz, W.H., Altherr, R., 2005. Noble gas isotopes suggest deep mantle plume source of late Cenozoic mafic alkaline volcanism in Europe. *Earth Planet. Sci. Lett.* 230, 143–162.
- Burnard, P.G., 2001. Correction for volatile fractionation in ascending magmas: noble gas abundances in primary mantle melts. *Geochim. Cosmochim. Acta* 65, 2605–2614.
- Burnard, P.G., 2004. Diffusive fractionation of noble gases and helium isotopes during mantle melting. *Earth Planet. Sci. Lett.* 220, 287–295.
- Craig, H., Lupton, J.E., 1976. Primordial neon, helium, and hydrogen in oceanic basalts. *Earth Planet. Sci. Lett.* 31, 369–385.
- Czuppon, G., Matsumoto, T., Handler, M., Matsuda, J., 2009. Noble gases in spinel peridotite xenoliths from Mt. Quincan, North Queensland, Australia: undisturbed MORB-type noble gases in the subcontinental lithospheric mantle. *Chem. Geol.* 266, 19–28.
- Demouchy, S., Jacobsen, S.D., Gaillard, F., Stern, C.R., 2006. Rapid magma ascent recorded by water diffusion profiles in mantle olivine. *Geology* 34, 429–432.
- Dodson, A., Brandon, A.D., 1999. Radiogenic helium in xenoliths from Simcoe, Washington, USA: implications for metasomatic processes in the mantle wedge above subduction zones. *Chem. Geol.* 160, 371–385.
- Doin, M.P., Fleitout, L., 1996. Thermal evolution of the oceanic lithosphere: an alternative view. *Earth Planet. Sci. Lett.* 142, 121–136.
- Fujiwara, T., Hirano, N., Abe, N., Takizawa, K., 2006. Subsurface structure of the "petit-spot" intra-plate volcanism in the northwestern Pacific. *JAMSTEC Rep. Res. Develop.* 3, 31–42.
- Fujiwara, T., Hirano, N., Abe, N., Takizawa, K., 2007. Subsurface structure of the "petit-spot" volcanoes on the northwestern Pacific Plate. *Geophys. Res. Lett.* 34, L13305. doi:10.1029/2007GL030439.
- Gaherty, J.B., Kato, M., Jordan, T.H., 1999. Seismological structure of the upper mantle: a regional comparison of seismic layering. *Phys. Earth Planet. Inter.* 110, 21–41.
- Gautheron, C., Moreira, M., Allègre, C., 2005. He, Ne and Ar composition of the European lithospheric mantle. *Chem. Geol.* 217, 97–112.
- Graham, D.W., 2002. Noble gas isotope geochemistry of mid-ocean ridge and ocean island basalts: characterization of mantle source reservoirs. In: Porcelli, D., Ballentini, C.J., Wieler, R. (Eds.), *Reviews in Mineralogy and Geochemistry: Noble Gases in Geochemistry and Cosmochemistry*, vol. 47. The Mineralogical Society of America, Washington, DC, pp. 247–317.
- Graham, D.W., Humphris, S.E., Jenkins, W.J., Kurz, M.D., 1992a. Helium isotope geochemistry of some volcanic rocks from Saint Helena. *Earth Planet. Sci. Lett.* 110, 121–131.
- Graham, D.W., Jenkins, W.J., Schilling, J.-G., Thompson, G., Kurz, M.D., Humphris, S.E., 1992b. Helium isotope geochemistry of mid-ocean ridge basalts from the South Atlantic. *Earth Planet. Sci. Lett.* 110, 133–147.
- Hanyu, T., Johnson, K.T.M., Hirano, N., Ren, Z.-Y., 2007. Noble gas and geochronology study of the Hana Ridge, Haleakala Volcano, Hawaii; implications to the temporal change of magma source and the structural evolution of the submarine ridge. *Chem. Geol.* 238, 1–18.
- Harrison, D., Barry, T., Turner, G., 2004. Possible diffusive fractionation of helium isotopes in olivine and clinopyroxene phenocrysts. *Eur. J. Mineral.* 16, 213–220.

- Heber, V.S., Brooker, R.A., Kelley, S.P., Wood, B.J., 2007. Crystal-melt partitioning of noble gases (helium, neon, argon, krypton, and xenon) for olivine and clinopyroxene. *Geochim. Cosmochim. Acta* 71, 1041–1061.
- Hirano, N., Kawamura, K., Hattori, M., Saito, K., Ogawa, Y., 2001. A new type of intraplate volcanism; young alkali-basalts discovered from the subducting Pacific Plate, northern Japan Trench. *Geophys. Res. Lett.* 28, 2719–2722.
- Hirano, N., Yamamoto, J., Kagi, H., Ishii, T., 2004. Young olivine xenocryst-bearing alkali-basalt from the oceanward slope of the Japan Trench. *Contrib. Mineral. Petrol.* 148, 47–54.
- Hirano, N., Takahashi, E., Yamamoto, J., Machida, S., Abe, N., Ingle, S., Kaneoka, I., Hirata, T., Kimura, J., Ishii, T., Ogawa, Y., Suyehiro, K., 2006. Volcanism in response to plate flexure. *Science* 313, 1426–1428.
- Hirano, N., Koppers, A.A.P., Takahashi, A., Fujiwara, T., Nakanishi, M., 2008. Seamounts, knolls and petit-spot monogenetic volcanoes on the subducting Pacific Plate. *Basin Res* 20, 543–553.
- Hirth, G., Kohlstedt, D.L., 1996. Water in the oceanic upper mantle: implications for rheology, melt extraction and the evolution of the lithosphere. *Earth Planet. Sci. Lett.* 144, 93–108.
- Hiyagon, H., Ozima, M., Marty, B., Zashu, S., Sakai, H., 1992. Noble gases in submarine glasses from mid-oceanic ridges and Loihi seamount: constraints on the early history of the Earth. *Geochim. Cosmochim. Acta* 56, 1301–1316.
- Holloway, J.R., 1998. Graphite-melt equilibrium during mantle melting: constraints on CO₂ in MORB magmas and the carbon content of the mantle. *Chem. Geol.* 147, 89–97.
- Honda, M., Patterson, D.B., 1999. Systematic elemental fractionation of mantle-derived helium, neon, and argon in mid-oceanic ridge glasses. *Geochim. Cosmochim. Acta* 63, 2863–2874.
- Hopp, J., Trieloff, M., Altherr, R., 2004. Neon isotopes in mantle rocks from the Red Sea region reveal large-scale plume–lithosphere interaction. *Earth Planet. Sci. Lett.* 219, 61–76.
- Hopp, J., Trieloff, M., Altherr, R., 2007a. Noble gas compositions of the lithospheric mantle below the Chyulu Hills volcanic field, Kenya. *Earth Planet. Sci. Lett.* 261, 635–648.
- Hopp, J., Trieloff, M., Buikin, A.I., Korochantseva, E.V., Schwarz, W.H., Althaus, T., Altherr, R., 2007b. Heterogeneous mantle argon isotope composition in the subcontinental lithospheric mantle beneath the Red Sea region. *Chem. Geol.* 240, 36–53.
- Jambon, A., Weber, H.W., Begemann, F., 1985. Helium and argon from an Atlantic MORB glass: concentration, distribution and isotopic composition. *Earth Planet. Sci. Lett.* 73, 255–268.
- Kaneoka, I., Takaoka, N., 1980. Rare gas isotopes in Hawaiian ultramafic nodules and volcanic rocks: constraint on genetic relationships. *Science* 208, 1366–1368.
- Karato, S., Jung, H., 1998. Water, partial melting and the origin of the seismic low velocity and high attenuation zone in the upper mantle. *Earth Planet. Sci. Lett.* 157, 193–207.
- Kawakatsu, H., Kumar, P., Takei, Y., Shinohara, M., Kanazawa, T., Araki, E., Suyehiro, K., 2009. Seismic evidence for sharp lithosphere–asthenosphere boundaries of oceanic plates. *Science* 324, 499–502.
- Kim, K.H., Nagao, K., Tanaka, T., Sumino, H., Nakamura, T., Okuno, M., Lock, J.B., Youn, J.S., Song, J., 2005. He–Ar and Nd–Sr isotopic compositions of ultramafic xenoliths and host alkali basalts from the Korean Peninsula. *Geochem. J.* 39, 341–356.
- Klügel, A., 1998. Reactions between mantle xenoliths and host magma beneath La Palma (Canary Islands): constraints on magma ascent rates and crustal reservoirs. *Contrib. Mineral. Petrol.* 131, 237–257.
- Kumagai, H., Kaneoka, I., 1998. Variations of noble gas abundances and isotope ratios in a single MORB pillow. *Geophys. Res. Lett.* 25, 3891–3894.
- Kumagai, H., Kaneoka, I., 2003. Relationship between submarine MORB glass textures and atmospheric component of MORBs. *Chem. Geol.* 200, 1–24.
- Kumagai, H., Kaneoka, I., 2005. Noble gas signatures around the Rodriguez Triple Junction in the Indian Ocean: constraints on magma genesis in a ridge system. *Geochim. Cosmochim. Acta* 69, 5567–5583.
- Kumagai, H., Dick, H.J.B., Kaneoka, I., 2003. Noble gas signatures of abyssal gabbros and peridotites at an Indian Ocean core complex. *Geochem. Geophys. Geosys.* 4 (12), 9107. doi:10.1029/2003GC000540.
- Kurz, M.D., 1986. Cosmogenic helium in a terrestrial igneous rock. *Nature* 320, 435–439.
- Kyser, T.K., Rison, W., 1982. Systematics of rare gas isotopes in basic lavas and ultramafic xenoliths. *J. Geophys. Res.* 87 (B7), 5611–5630.
- Leya, I., Wieler, R., 1999. Nucleogenic production of Ne isotopes in Earth's crust and upper mantle induced by alpha particles from the decay of U and Th. *J. Geophys. Res.* 104, 15439–15450.
- Macpherson, C.G., Hilton, D.R., Mertz, D.F., Dunai, T.J., 2005. Source, degassing, and contamination of CO₂, H₂O, He, Ne, and Ar in basaltic glasses from Kolbeinsey Ridge, North Atlantic. *Geochim. Cosmochim. Acta* 69, 5729–5746.
- Marty, B., 1989. Neon and xenon isotopes in MORB: implications for the earth-atmosphere evolution. *Earth Planet. Sci. Lett.* 94, 45–56.
- Marty, B., Ozima, M., 1986. Noble gas distribution in oceanic basaltic glasses. *Geochim. Cosmochim. Acta* 50, 1093–1097.
- Matsuda, J., Marty, B., 1995. The ⁴⁰Ar/³⁶Ar ratio of the undepleted mantle; a reevaluation. *Geophys. Res. Lett.* 22, 1937–1940.
- Matsumoto, T., Honda, M., McDougall, I., O'Reilly, S.Y., 1998. Noble gases in anhydrous lherzolites from the Newer Volcanics, southeastern Australia: a MORB-like reservoir in the subcontinental mantle. *Geochim. Cosmochim. Acta* 62, 2521–2533.
- Matsumoto, T., Honda, M., McDougall, I., O'Reilly, S.Y., Norman, M., Yaxley, G., 2000. Noble gases in pyroxenites and metasomatised peridotites from the Newer Volcanics, southeastern Australia: implications for mantle metasomatism. *Chem. Geol.* 168, 49–73.
- Matsumoto, T., Chen, Y., Matsuda, J., 2001. Concomitant occurrence of primordial and recycled noble gases in the Earth's mantle. *Earth Planet. Sci. Lett.* 185, 35–47.
- Matsumoto, T., Morishita, T., Matsuda, J., Fujioka, T., Takebe, M., Yamamoto, K., Arai, S., 2005. Noble gases in the Finero phlogopite-peridotites, western Italian Alps. *Earth Planet. Sci. Lett.* 238, 130–145.
- Milashiev, V.A., 1988. *Explosion Pipes*. Springer-Verlag, New York. 249 pp.
- Moreira, M., Sarda, P., 2000. Noble gas constraints on degassing processes. *Earth Planet. Sci. Lett.* 176, 375–386.
- Moreira, M., Allègre, C.J., 2002. Rare gas systematics on Mid-Atlantic Ridge (37–40N). *Earth Planet. Sci. Lett.* 198, 401–416.
- Moreira, M., Staudacher, T., Sarda, P., Schilling, J.G., Allègre, C.J., 1995. A primitive plume neon component in MORB: the Shona Ridge anomaly, South Atlantic (51–52S). *Earth Planet. Sci. Lett.* 133, 367–377.
- Moreira, M., Valbracht, P.J., Staudacher, T., Allègre, C.J., 1996. Rare gas systematics in Red Sea ridge basalts. *Geophys. Res. Lett.* 23, 2453–2456.
- Moreira, M., Kunz, J., Allègre, C.J., 1998. Rare gas systematics in popping rock: isotopic and elemental compositions in the upper mantle. *Science* 279, 1178–1181.
- Neumann, E.-R., Wulff-Pedersen, E., 1997. The origin of highly silicic glass in mantle xenoliths from the Canary Islands. *J. Petrol.* 38, 1513–1539.
- Neumann, E.-R., Sorensen, V.B., Simonsen, S.L., Johnsen, K., 2000. Gabbroic xenoliths from La Palma, Tenerife and Lanzarote, Canary Islands: evidence for reactions between mafic alkaline Canary Islands melts and old oceanic crust. *J. Vol. Geotherm. Res.* 103, 313–342.
- Neumann, E.-R., Wulff-Pedersen, E., Pearson, N.J., Spencer, E.A., 2002. Mantle xenoliths from Tenerife (Canary Islands): evidence for reactions between mantle peridotites and silicic carbonatite melts inducing Ca metasomatism. *J. Petrol.* 43, 825–857.
- Niedermann, S., Bach, W., 1998. Anomalously nucleogenic neon in North Chile Ridge basalt glasses suggesting a previously degassed mantle source. *Earth Planet. Sci. Lett.* 160, 447–462.
- Niedermann, S., Bach, W., Erzinger, J., 1997. Noble gas evidence for a lower mantle component in MORBs from the southern East Pacific Rise: decoupling of helium and neon isotope systematics. *Geochim. Cosmochim. Acta* 61, 2697–2715.
- Nishimoto, S., 1996. Modal analysis of granitic rocks by a personal computer using image processing software "Adobe photoshop™". *J. Min. Pet. Econ. Geol.* 91, 235–241.
- Nuccio, P.M., Paonita, A., Rizzo, A., Rosciglione, A., 2008. Elemental and isotope covariation of noble gases in mineral phases from Etna volcanics erupted during 2001–2005, and genetic relation with peripheral gas discharges. *Earth Planet. Sci. Lett.* 272, 683–690.
- O'Neill, H., 1981. The transition between spinel lherzolite and garnet lherzolite, and its use as a geobarometer. *Contrib. Mineral. Petrol.* 77, 185–194.
- Ozima, M., Podosek, F.A., 1983. *Noble Gas Geochemistry*. Cambridge University Press, Cambridge.
- Ozima, M., Zashu, S., 1983. Noble gases in submarine pillow volcanic glasses. *Earth Planet. Sci. Lett.* 62, 24–40.
- Parman, S.W., Kurz, M.D., Hart, S.R., Grove, T.L., 2005. Helium solubility in olivine and implications for high ³He/⁴He in ocean island basalts. *Nature* 437, 1140–1143.
- Patterson, D.B., Honda, M., McDougall, I., 1994. Noble gases in mafic phenocrysts and xenoliths from New Zealand. *Geochim. Cosmochim. Acta* 58, 4411–4427.
- Peslier, A.H., Luhr, J.F., 2006. Hydrogen loss from olivines in mantle xenoliths from Simcoe (USA) and Mexico: mafic alkaline magma ascent rates and water budget of the sub-continental lithosphere. *Earth Planet. Sci. Lett.* 242, 302–319.
- Presnell, D.C., Gudfinnsson, G.H., Walter, M.J., 2002. Generation of mid-ocean ridge basalts at pressures from 1 to 7 GPa. *Geochim. Cosmochim. Acta* 66, 2073–2090.
- Resing, J.A., Lupton, J.E., Feely, R.A., Lilley, M.D., 2004. CO₂ and ³He in hydrothermal plumes: implications for mid-ocean ridge CO₂ flux. *Earth Planet. Sci. Lett.* 226, 449–464.
- Sarda, P., Staudacher, T., Allègre, C.J., 1988. Neon isotopes in submarine basalts. *Earth Planet. Sci. Lett.* 91, 73–88.
- Sarda, P., Moreira, M., Staudacher, T., Schilling, J.-G., Allègre, C.J., 2000. Rare gas systematics on the southernmost Mid-Atlantic Ridge: constraints on the lower mantle and the Dupal source. *J. Geophys. Res.* 105, 5973–5996.
- Shimamura, H., Asada, T., 1984. Velocity anisotropy extending over the entire depth of the oceanic lithosphere. In: Hilde, T.W.C., Uyeda, S. (Eds.), *Geodynamics Ser.*, vol. 11. Am. Geophys. Union, pp. 121–125.
- Shuster, D.L., Farley, K.A., 2005. Diffusion kinetics of proton-induced ²¹Ne, ³He, and ⁴He in quartz. *Geochim. Cosmochim. Acta* 69, 2349–2359.
- Song, S., Su, L., Niu, Y., Lai, Y., Zhang, L., 2009. CH₄ inclusions in orogenic harzburgite: evidence for reduced slab fluids and implication for redox melting in mantle wedge. *Geochim. Cosmochim. Acta* 73, 1737–1754.
- Spera, F.J., 1984. Carbon dioxide in petrogenesis III: role of volatiles in the ascent of alkaline magma with special reference to xenolith-bearing mafic lavas. *Contrib. Mineral. Petrol.* 88, 217–232.
- Staudacher, T., Sarda, P., Richardson, S.H., Allègre, C.J., Sagna, I., Dmitriev, L.V., 1989. Noble gases in basaltic glasses from a Mid-Atlantic Ridge topographic high at 14°N: geodynamic consequences. *Earth Planet. Sci. Lett.* 96, 119–133.
- Stein, C.A., Stein, S., 1992. A model for the global variation in oceanic depth and heat flow with lithospheric age. *Nature* 359, 123–129.
- Stroncik, N.A., Niedermann, S., Haase, K.M., 2008. Plume–ridge interaction revisited: evidence for melt mixing from He, Ne and Ar isotope and abundance systematics. *Earth Planet. Sci. Lett.* 268, 424–432.
- Takahashi, E., 1986. Origin of basaltic magmas – implications from peridotite melting experiments and an olivine fractionation model. *Bull. Volcanol. Soc. Japan* 30, 17–40.
- Trull, T.W., Kurz, M.D., 1993. Experimental measurements of ³He and ⁴He mobility in olivine and clinopyroxene at magmatic temperatures. *Geochim. Cosmochim. Acta* 57, 1313–1324.
- Trull, T.W., Kurz, M.D., 1999. Isotopic fractionation accompanying helium diffusion in basaltic glass. *J. Mol. Struct.* 485–486, 555–567.

- Vance, D., Stone, J.O.H., O'Nions, R.K., 1989. He, Sr and Nd isotopes in xenoliths from Hawaii and other oceanic islands. *Earth Planet. Sci. Lett.* 96, 147–160.
- Wakita, H., Nagasawa, H., Uyeda, S., Kuno, H., 1967. Uranium, thorium and potassium contents of possible mantle materials. *Geochem. J.* 1, 183–198.
- Wells, P.R.A., 1977. Pyroxene thermometry in simple and complex systems. *Contrib. Mineral. Petrol.* 62, 129–139.
- Wetherill, G.W., 1954. Variations in the isotopic abundances of neon and argon extracted from radioactive minerals. *Phys. Rev.* 96, 679–683.
- Yamamoto, J., Hirano, N., Hanyu, T., Kagi, H., Kaneoka, I., 2003. Noble gases in mantle-derived xenocrysts in an alkali basalt from Japan Trench oceanward slope. In: Vladkyin, N.V. (Ed.), *Plume and Problems of Deep Sources of Alkaline Magmatism*. Irkutsk State Technical University, Irkutsk, pp. 39–50.
- Yamamoto, J., Kaneoka, I., Nakai, S., Kagi, H., Prikhod'ko, V.S., Arai, S., 2004. Evidence for subduction-related components in the subcontinental mantle from low $^3\text{He}/^4\text{He}$ and $^{40}\text{Ar}/^{36}\text{Ar}$ ratio in mantle xenoliths from Far Eastern Russia. *Chem. Geol.* 207, 237–259.
- Yamamoto, J., Nishimura, K., Sugimoto, T., Takemura, K., Takahata, N., Sano, Y., 2009a. Diffusive fractionation of noble gases in mantle with magma channels: origin of low He/Ar in mantle-derived rocks. *Earth Planet. Sci. Lett.* 280, 167–174.
- Yamamoto, J., Nakai, S., Nishimura, K., Kaneoka, I., Kagi, H., Sato, K., Okumura, T., Prikhod'ko, V.S., Arai, S., 2009b. Intergranular trace elements in mantle xenoliths from the Russian Far East: an example for mantle metasomatism by hydrous melt. *The Island Arc* 18, 225–241.
- Yatsevich, I., Honda, M., 1997. Production of nucleogenic neon in the Earth from natural radiogenic decay. *J. Geophys. Res.* B5, 10291–10298.